พฤติกรรมการเปลี่ยนรูปร่างแบบวงรอบของโลหะเชื่อมดีบุก-เงิน-ทองแดง-บีสมัธ

Cyclic deformation behavior of Sn-Ag-Cu-Bi solder

ชาวสวน กาญจโนมัย

Chaosuan Kanchanomai

บทคัดย่อ

โลหะเชื่อมยูเทกติกดีบุก-เงิน (Sn-3.5Ag) และโลหะเชื่อมดีบุก-เงิน-ทองแดง-บีสมัธ (Sn-3Ag-0.5Cu-3Bi) ที่ใช้ในอุปกรณ์อิเล็กทรอนิกส์ ได้ถูกทำการทดสอบการล้าแบบจำนวนรอบต่ำ (low cycle fatigue, LCF) เพื่อศึกษาถึงผลกระทบของการเติมทองแดง และบีสมัธที่มีต่อพฤติกรรมการเปลี่ยนรูปร่างแบบวงรอบ (cyclic deformation), แถบเลื่อน (slip band) และอายุการใช้งาน ผลการทดลองพบว่าความเครียดในโลหะเชื่อมยูเทกติกดีบุก-เงินลดลงเมื่อเพิ่มจำนวนรอบ เนื่องมาจากการเกิดรอยร้าว ในขณะที่โลหะเชื่อมดีบุก-เงิน-ทองแดง-บีสมัธแสดงการเพิ่มของความเครียดในระยะเริ่มต้น ตามด้วยการลดลงของความเครียดเมื่อเพิ่มจำนวนรอบ เนื่องจากผลกระทบซึ่งกันและกันระหว่างดิสโลเคชัน (dislocation) และอนุภาคบีสมัธในดีบุก พฤติกรรมการล้าของโลหะเชื่อมทั้งสองแสดงความสัมพันธ์แบบคอฟฟิน-แมนซั่น (Coffin-Manson relationship) โดยอายุการล้า (fatigue life) ของโลหะเชื่อมดีบุก-เงิน-ทองแดง-บีสมัธแสดงมีค่าต่ำกว่าโลหะเชื่อมยูเทกติกดีบุก-เงิน

ABSTRACT

LCF tests on as-cast Sn-Ag eutectic solder (Sn-3.5Ag) and Sn-Ag-Cu-Bi solder (Sn-3Ag-0.5Cu-3Bi) have been performed to study the effects of additional Cu and Bi on the cyclic deformation behavior, slip band and reliability. For Sn-3.5Ag, the pattern of variation of stress amplitude with cycling showed a rapid decrease followed by slow rate of softening before instability sets in. The cracking due to cycling contributed to the reduction in stress amplitude. On the other hand, Sn-3Ag-0.5Cu-3Bi exhibited initial hardening followed by softening. The initial hardening is considered to arise from the interaction of dislocations with Bi-precipitates formed in dendrite phase. The LCF behavior of both solders followed the Coffin-Manson equation. However, fatigue life of Sn-3Ag-0.5Cu-3Bi was significantly lower compared to that of Sn-3.5Ag.

INTRODUCTION

In the surface mount technology (SMT) developed for electronic packaging, devices are directly soldered to pads on both sides of a printed wiring board (PWB). This technology allows placement of more surface mount components (SMC) into smaller and tighter printed wiring board areas. However, there are environmental and health concerns about the hazard of lead contained in conventional solder materials. Lead-free Sn-Ag system solders are candidates for electronic

---

ภาควิชาวิศวกรรมเครื่องกล, คณะวิศวกรรมศาสตร์, มหาวิทยาลัยธรรมศาสตร์, ปทุมธานี 12121 ประเทศไทย

Department of Mechanical Engineering, Thammasat University, Pathumthani 12121, Thailand

Tel: +66-02-564-3001; Fax: +66-02-564-3010, E-mail: kchao@engr.tu.ac.th

packaging. The mechanical properties and reliability of the Sn-Ag eutectic solder compare favorably with those of the Sn-Pb eutectic solder, while the solderability and melting temperature are less favorable than those of Sn-Pb eutectic solder (Kang and Sarkhel, 1994). In order to improve these properties, some additional elements, e.g. Cu, Bi, Zn, In, have been added to Sn-Ag eutectic solder. It has been reported that the melting temperature, i.e. liquidus and solidus temperatures, of Sn-Ag eutectic could be decreased by adding Bi or Zn (Hua and Glazer, 1997; McCormack and Jin, 1993). However, very little is known about the effects of additional elements on the cyclic deformation behavior, slip band and reliability of Sn-Ag eutectic solder. Kanchanomai et al. (2002a) found that the pattern of variation of stress amplitude with cycling showed a rapid decrease followed by slow rate of softening before instability sets in for the low cycle fatigue (LCF) study of Sn-3.5Ag, Sn-3Ag-0.5Cu and Sn-3Ag-0.5Cu-1Bi solders. On the other hand, Sn-3Ag-0.5Cu-3Bi exhibited initial hardening followed by softening at high strain ranges. Kariya and Otsuka (1998a, 1998b) reported that fatigue life of Sn-3.5Ag-Bi for a total axial strain-controlled test decreased with increasing contents of Bi (between 0-10 wt%), while addition of Cu (between 0-2 wt%) had no effect on the fatigue properties of Sn-3.5Ag-Cu. This reduction is attributed to the decrease in ductility with Bi addition and the presence of irregularly shaped Ag_3Sn in the microstructure.

In the present study, isothermal LCF tests on as-cast Sn-Ag eutectic solder (Sn-3.5Ag) and Sn-Ag-Cu-Bi solder (Sn-3Ag-0.5Cu-3Bi) were carried out to study the effects of additional elements on the cyclic deformation behavior, slip band and reliability. It is discussed in the paper that the interaction of dislocations with Bi-precipitates causes the initial cyclic hardening and the decrease in ductility, which consequently leads to lower fatigue life.

MATERIALS AND EXPERIMENTAL PROCEDURE

Sn-3.5Ag and Sn-3Ag-0.5Cu-3Bi alloys, were supplied in as-solidified form. Additions of Cu and Bi reduced the melting temperature of solders when compared to Sn-Ag eutectic solder, i.e. from 221 ^{o}C to 207 ^{o}C (Kanchanomai et al., 2002a). For observation of the microstructures, the solders were etched with 10g of $FeCl_3$, 2ml of HCl and 100ml of distilled water. SEM micrographs of the alloys are shown in Fig. 1. For Sn-3.5Ag alloy, β-Sn phase is the major phase, which comprises over 90% by volume. Its microstructure can be characterized by primary β-Sn dendrites (dark) and Sn-Ag eutectic phases (light), which comprise of some needles and particles of Ag_3Sn together within the Sn-rich matrix. Similar microstructures are observed for Sn-3Ag-0.5Cu-3Bi, however both Ag_3Sn and Cu_6Sn_5 form in the Sn-Ag-Cu eutectic phases (light). According to the binary phase diagrams of Sn-Ag and Sn-Cu (Lyman, 1973), the solubility of Ag and Cu in Sn-rich phase at eutectic and room temperature is negligible. On the other hand, from the binary phase diagram of Sn-Bi (Lyman, 1973), approximately 1-wt% and 21-wt% of Bi can dissolve in the Sn-rich matrix at room temperature and eutectic temperature (139 °C), respectively. Therefore, the dendrite phase in Sn-3Ag-0.5Cu-3Bi solder is essentially the precipitates of Bi in the solid solution Bi-Sn.

(a) 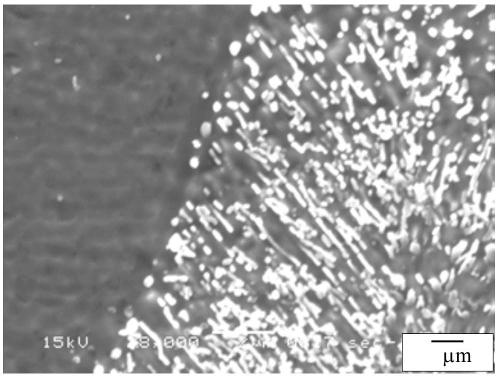

(b) 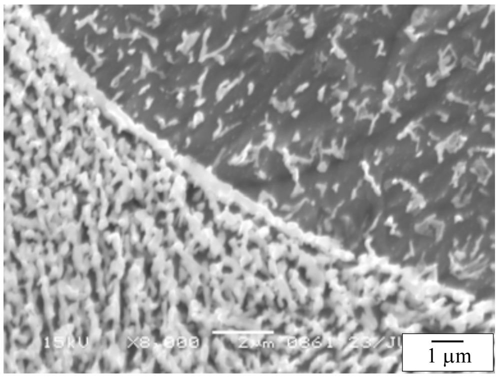

Fig. 1 SEM micrographs of (a) Sn-3.5Ag eutectic solder and (b) Sn-3Ag-0.5Cu-3Bi solder.

Monotonic tensile tests were conducted in order to understand the basic mechanical properties. Round specimens with a diameter of 7 mm and a gage length of 20 mm were used for the tests. For the present study, the strain rate of 4×10^{-2} s^{-1} was used for the tensile tests at 20 °C. The mechanical properties of the solders studied are summarized in Table 1.

Table 1 Mechanical properties of lead-free solders.

Solder	Young's modulus (GPa)	Yield strength (MPa)	Tensile strength (MPa)	True fracture ductility (D)	Hardness
Sn-3.5Ag	50	18.9	37.5	1.6	11.0 HV
Sn-3Ag-0.5Cu-3Bi	53	38.1	91.3	0.36	28.6 HV
Sn	41.6[a]	-	-	-	3.9 HB[a]
Bi	32[a]	-	-	-	7 HB[a]

[a] Cubberly, 1979

From bulk solder bar materials, fatigue specimens were machined on an NC lathe machine. The configuration of the specimen, which was designed according to the ASTM E606 (1998), has a diameter of 12 mm at the two ends, a center diameter of 6 mm, and a gage length of 9 mm. The total strain controlled fatigue tests were performed by using a servo-hydraulic fatigue machine under 55 % relative humidity and a constant temperature of 20 °C. In order to avoid the local deformation and stress concentration at contact point induced by the conventional displacement-measuring device, a digital image measurement system (Kanchanomai et al., 2002b) was used in the present strain-controlled fatigue test. A triangular waveform with 0.1 Hz frequency and R=-1 strain ratio was used for the fatigue tests. The cycle loading was started from tensile side. The fatigue failure was defined as 25% reduction of maximum tensile load (JSMS, 2000).

RESULTS AND DISSCUSSION

Cyclic deformation behavior

Both the load signal from load cell and the displacement signal from digital image system were recorded in a personal computer and then were used for calculating cyclic stress and strain in each cycle. Stress-strain hysteresis loops of both solders at the first cycle for 1.5% total strain range are shown in Fig. 2. For Sn-3Ag-0.5Cu-3Bi solder, the stress range was higher while the plastic strain range was lower compared to those of Sn-3.5Ag. These results correspond to a greater tensile strength and microhardnesses measured for Sn-Ag-Cu-Bi alloys. The plastic strain range increased with the applied total strain range but did not vary with the number of cycles for alloys investigated. In the present study, a small decrease in plastic strain range for a few initial cycles was observed in the case of Sn-3Ag-0.5Cu-3Bi solder, particularly at high strain ranges.

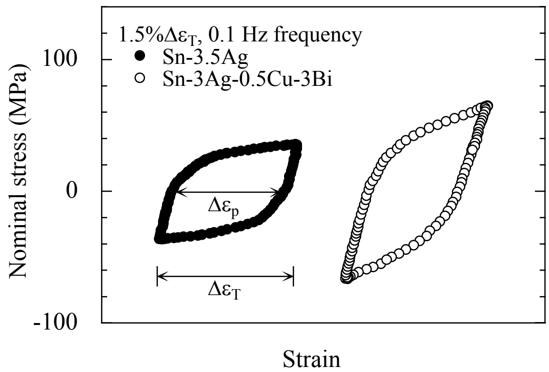

Fig. 2 Cyclic stress-strain hysteresis loops at the beginning of fatigue tests.

The relationships between stress amplitude (one-half of the stress range) and number of cycles for both solders are shown in Fig. 3. Cyclic softening was observed for Sn-3.5Ag from the beginning of the tests. On the other hand, Sn-3Ag-0.5Cu-3Bi exhibited higher stress amplitude with initial hardening, and followed by relatively faster rate of softening compared to the Sn-Ag eutectic solder.

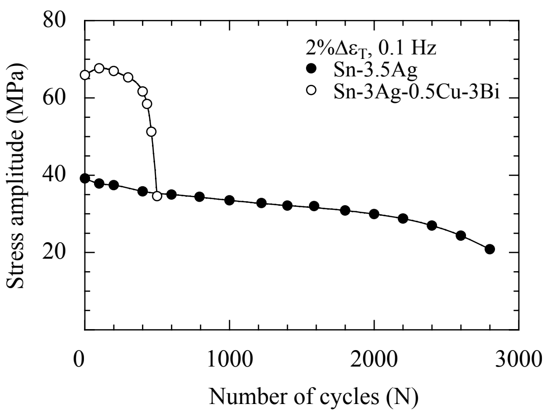

Fig. 3 Relationship between stress amplitudes and number of cycles.

The observed cyclic flow behavior is consistent with the microstructural features of the alloys. The initial rapid decrease followed by a slower rate of decrease of stress amplitude in Sn-3.5Ag has been attributed to development of extensive surface cracking along β-Sn dendrite boundaries, their linking up and propagation transgranularly through the Sn-Ag eutectic phase and intergranularly along Sn-dendrite and/or subgrain boundaries at this test frequency (Kanchanomai et al., 2002c). The presence of Cu in Sn-3Ag-0.5Cu-3Bi solder introduces Cu_6Sn_5 precipitates in the eutectic phase and this is responsible for the higher stress amplitude observed for this material compared to Sn-3.5Ag. Moreover, the addition of 3% Bi in this solder would essentially form Bi-precipitate and solid solution of Bi in β-Sn dendrite at room temperature and leads to strengthening of this phase. As β-Sn comprises about 90% of the volume fraction in this material, precipitate and solid solution strengthening by Bi are expected to increase stress amplitude and decrease plastic strain range as observed.

Apart from the higher stress response, there is clearly initial hardening observed, particularly at large strain amplitudes, followed by softening for Sn-3Ag-0.5Cu-3Bi. This material, in addition to solid solution hardening of β-Sn dendrites, contains precipitates of Bi. The initial hardening is, therefore, attributed to the presence of Bi precipitates and arises from the interaction of dislocations with these precipitates. It is known that the precipitations from supersaturated solid solutions frequently have interphase boundaries that are coherent with the matrix (Courtnry, 1990), therefore the precipitates of Bi in Sn-rich matrix are considered to be coherent particles for the present Sn-3Ag-0.5Cu-3Bi solder. Normally, second-phase particles, which have coherent boundaries with the matrix, act in two different manners to retard the motion of dislocations. The particles either may be cut by the dislocations or the particles resist cutting and then dislocations are forced to bypass them. For small and soft particles, dislocations can cut and deform the particles. Particles, which are sheared by dislocations, tend to produce planar and coarse slip (Fig. 4a). On the other hand, the cutting of particles becomes difficult for high strength particles and instead the dislocations find ways of moving around the particles (dislocation looping), as shown in Fig. 4b. Moreover, dislocation looping is enhanced for large coherent particles (high particle spacing). In this condition, slips are very short or indistinct, and secondary slip system can be observed (Dieter, 1986).

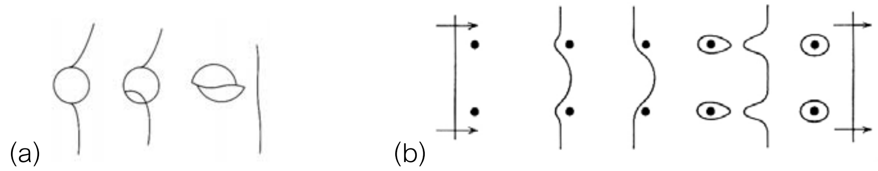

Fig. 4 Dislocation-particle interaction: (a) dislocation cutting through a particle, and (b) dislocation moving around a particle (Dieter, 1986).

In many commercial alloys, typical sizes of particle, at which the transition from dislocation cutting through a particle to dislocation moving around a particle occurs, are in the range of 10-20 nm (Courtney, 1990). Since the size of Bi precipitates for the present Sn-3Ag-0.5Cu-3Bi solder is approximately 0.5-1 μm (Fig. 1b), Bi has higher strength comparing to Sn (Table 1), and dislocation mobility is high for Sn, i.e. element with high stacking fault energy (Hardwick, 1961), the cutting of dislocations through the solute-Bi is unlikely the hardening mechanism observed here. Moreover, fine-wavy slips with secondary slip system were observed in the dendrite phases of Sn-3Ag-0.5Cu-3Bi, while coarse-wavy slips were observed in dendrite phases of Sn-3.5Ag, as shown in Fig. 5. It is likely that dislocation looping around Bi particles is the cyclic hardening mechanism for the present Sn-3Ag-0.5Cu-3Bi. Orowan (1947) proposed that a dislocation loop is left around each particle when dislocation moves around the particle. If news dislocation lines come along, each can repeat this process and leave a new dislocation loop around the obstacles. These loops exert a back stress on dislocation sources, which must be overcome for additional slip to take place. This requires an increase in flow stress, i.e. strain hardening. The degree of hardening depends on a number of parameters, e.g. volume fraction of second-phase particles, strain, material properties, temperature, rate of recovery process (Schmidt and Miller, 1982). Increasing strain and volume fraction of additional Bi tend to induce more dislocations and resistance of dislocation movement, which consequently enhance the hardening behavior. It should be noted that during the tests (20 °C, about 0.6 of absolute melting temperature of both solders), not only hardening process occurs, but recovery process, i.e. polygonization and recrystallization, and fatigue damage also play an important role (Kanchanomai et al., 2002a,c). Therefore, more study is needed in order to fully understand the cyclic deformation behavior of this solder.

(a) (b)

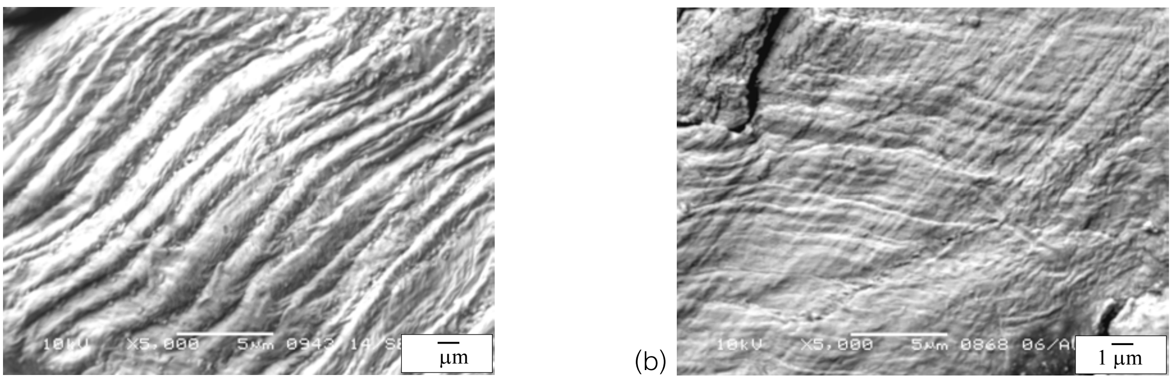

Fig. 5 SEM micrograph of surface of failed specimens tested at 1%$\Delta\varepsilon_T$, 0.1 Hz, (a) Sn-3.5Ag: evidence of coarse-wavy slips appeared in the dendrite phase, (b) Sn-3Ag-0.5Cu-3Bi solder: evidence of fine-wavy slips with secondary slip system appeared in the dendrite phase (load direction in vertical).

Fatigue life

It is well known that relationship between plastic strain range and number of cycles to failure follows the Coffin-Manson relationship (Coffin, 1954; Manson, 1953).

$$\Delta\varepsilon_p N_f^{\alpha} = \theta \qquad (1)$$

where $\Delta\varepsilon_p$ is plastic strain range, N_f is fatigue life, α is fatigue ductility exponent and θ is fatigue ductility coefficient. The Coffin-Manson relationships for both solders are shown in Fig. 6. Both solders obey the Coffin-Manson relationship with correlation coefficient in the range of 0.97-0.99. Fatigue ductility exponent (α) of both are basically similar, while the fatigue ductility coefficient (θ) is higher for Sn-3.5Ag solder.

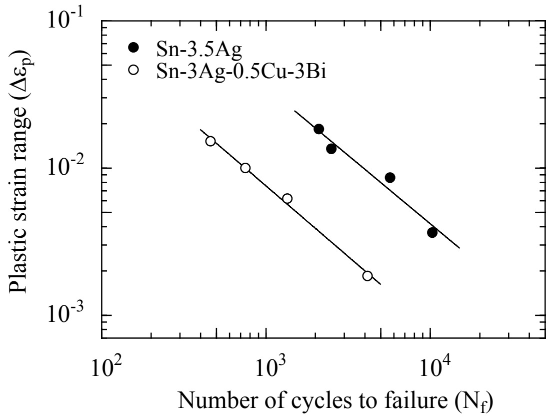

Fig. 6 Relationship between plastic strain range and number of cycles to failure.

It is suggested that lower ductility and lower life observed for solder with Bi addition arises due to strengthening of Sn-dendrite with solid solution of Bi as well as precipitates. The presence of Bi precipitates in Sn-rich phase leads to the formation of cavities (Kanchanomai et al., 2002a) and also probably contributed to decrease in fatigue life. The high response stresses observed for solder with Bi addition would be another reason for reduced fatigue life as observed.

CONCLUSIONS

Isothermal LCF tests on as-cast Sn-Ag eutectic solder (Sn-3.5Ag) and Sn-Ag-Cu-Bi solder (Sn-3Ag-0.5Cu-3Bi) have been performed at 20 ^{o}C with a constant frequency of 0.1 Hz to study the effects of additional elements on the cyclic deformation behavior, slip band and reliability. The main conclusions obtained are summarized as follows:

1) For Sn-3.5Ag, the pattern of variation of stress amplitude with cycling showed a rapid decrease followed by slow rate of softening before instability sets in. The surface cracking, link-up and propagation due to cycling contributed to the reduction in stress amplitude. On the other hand, Sn-3Ag-0.5Cu-3Bi exhibited initial hardening followed by softening. The initial hardening is considered to arise from the interaction of dislocations with Bi-precipitates formed in dendrite phase.

2) Fine-wavy slips with secondary slip system were observed in the dendrite phases of Sn-3Ag-0.5Cu-3Bi, while coarse-wavy slips were observed in dendrite phases of Sn-3.5Ag. It is likely that dislocation looping around Bi particles is the cyclic hardening mechanism for Sn-3Ag-0.5Cu-3Bi.
3) The LCF behavior of both solders followed the Coffin-Manson equation. However, fatigue life was significantly lower for solder with the addition Bi and Cu compared to that of Sn-3.5Ag.

REFFERENCES

ASTM standards, 1998. ASTM E606: Standard Practice for Strain-Controlled Fatigue Testing. The American Society for Testings and Materials, Vol. 03.01 : 525-539.

Coffin, L.F., Jr. 1954. A study of the Effects of Cyclic Thermal Stresses on a Ductile Metal. Trans. of ASME. 76 : 931-50.

Courtney, T.H. 1990. Mechanical Behavior of Materials. McGraw-Hil : 184-214.

Cubberly, W.H. 1979. editor, Metals Handbook, 9th edition, Vol. 2, American Society for Metals, Metals Park, Ohio 44073, p. 618, 719.

Dieter, G.E. 1986. Mechanical Metallurgy, McGraw-Hill, New York, pp. 184-240.

Hardwick, D., C.M. Sellars, and W.J. McG. Tegart. 1961-1962. The Occurrence of Recrystallization During High-Temperature Creep. J. Inst. Metals. 90 : 21-22.

Hua, F. and J. Glazer. 1997. Lead-free solders for electronic assembly, design and reliability of solders and solder interconnections, in: R.K. Mahidhara, D.R. Frear, S.M.L. Sastry, K.L. Liaw, W.L. Winterbottom (Eds.), The Minerals, Metals and Materials Society, 1997, pp. 65-74.

JSMS Standards. 2000. JSMS-SD-3-00: Standard Method for Low Cycle Fatigue Testing of Solder Materials. The Society of Material Science, Japan.

Kanchanomai, C., Y. Miyashita and Y. Mutoh. 2002a. Low Cycle Fatigue Behavior of Sn-Ag, Sn-Ag-Cu and Sn-Ag-Cu-Bi Lead-free Solders. J. Electron. Mater. 31(5) : 456-65.

Kanchanomai, C., S. Yamamoto, Y. Miyashita, Y. Mutoh and A.J. McEvily. 2002b. Low Cycle Fatigue Test for Solders Using Non-Contact Digital Image Measurement System. Inter. J. Fatigue. 24(1) : 57-67.

Kanchanomai, C., Y. Miyashita, Y. Mutoh and S.L. Mannan. 2002c. Influence of Frequency on Low Cycle Fatigue Behavior of Sn-Ag Eutectic Solder. Mater. Sci. Engr. A, in press.

Kang, S.K. and A.K. Sarkhel. 1994. Lead (Pb)–Free Solders for Electronic Packaging. J. Electron. Mater. 23(8) : 701-7.

Kariya, Y. and M. Otsuka. 1998a. Mechanical Fatigue Characteristics of Sn-3.5Ag-x (x = Bi, Cu, Zn and In) Solder Alloys. J. Electron. Mater. 27(11) : 1229-35.

Kariya Y, and M. Otsuka. 1998b. Effect of Bismuth on the Isothermal Fatigue Properties of Sn-3.5mass%Ag Solder Alloy. J. Electron. Mater. 27 : 866-70.

Lyman, T. 1973, editor, Metals Handbook, 8th edition, Vol. 8, American Society for Metals, Metals Park, Ohio 44073, p. 256, 273, 299.

Manson SS. 1953. Behavior of Materials Under Conditions of Thermal Stress. Heat Transfer Symposium. University of Michigan. University of Michigan Press, pp. 9-76.

McCormack, M. and S. Jin. 1993. JOM 45(7) : 36.

Orowan, E. 1947. Discussion, Symposium on Internal Stresses, Institute of Metals, London, p. 451.

Schmidt, C.G. and A.K. Miller. 1982. The Effect of Solutes on the Strength and Strain Hardening Behavior of Alloys. Acta Metallurgica. 30 : 615-25.